DEVELOPMENT OF NITINOL ALLOYS FOR ADDITIVE MANUFACTURING

Kerri M. Horvay, Christopher T. Schade

Hoeganaes Specialty Metal Powders LLC.
Cinnaminson, NJ 08077

Keywords: Additive Manufacturing, SLM, Nitinol, Transformation Temperature

Abstract

Nickel-titanium (Nitinol) shape memory alloys exhibit unique properties, such as the shape memory effect and superelasticity. The shape memory effect occurs when the alloy is deformed in the martensitic state then heated above its transformation temperature where it reverts to austenite and returns to its original shape. The role of gas atomization parameters, chemical composition, and particle size distribution of Nitinol powder are studied in relation to the transformation temperature. Typical particle sizes utilized in selective laser melting (SLM) and directed energy deposition (DED) additive manufacturing (AM) processes are examined. The influence of re-melting the powder and the subsequent solidification effects, as would be seen in SLM, are studied in relation to the transformation temperature.

Introduction

Nitinol, a near-equiatomic alloy of nickel and titanium, has numerous current applications (e.g., automotive, aerospace, biomedical, actuators, and sensors) due to its shape memory properties and superelasticity, but there are many challenges to overcome concerning manufacturing and processing [1]. From a powder production point of view, the influence of post-processing on the transformation temperature needs to be fully understood to provide a customer with the correct starting material for their application.

The shape memory effect (SME) refers to a material's ability to recover its original shape by heating after it has been plastically deformed. The low temperature phase where it is deformed is martensite and the high temperature phase to which it is heated to is austenite. The temperatures where these transformations begin and end are termed: austenite start (A_s), austenite finish (A_f), martensite start (M_s), and martensite finish (M_f). Superelasticity is exhibited when a material is mechanically loaded in the austenitic phase, causing it to transform to stress induced martensite and when the load is released the material transforms back to austenite and its original shape [1].

The production of Nitinol is very difficult. The elastic response and the SME are closely tied to the chemical composition. Small changes in the level of nickel or titanium can have large effects on these properties (Figure 1). The accuracy of measuring the nickel and titanium concentrations at such high levels is generally an issue (resolution of +/-0.10%) and many suppliers of Nitinol metal certify their material to a transformation temperature rather than the chemical composition [2]. In addition to the tight compositional control required to make this alloy, the reactivity (oxidation) of titanium and volatility of nickel during the melting process

make predicting the A_f temperature very challenging. When converting the solid metal to a powder there are further complications.

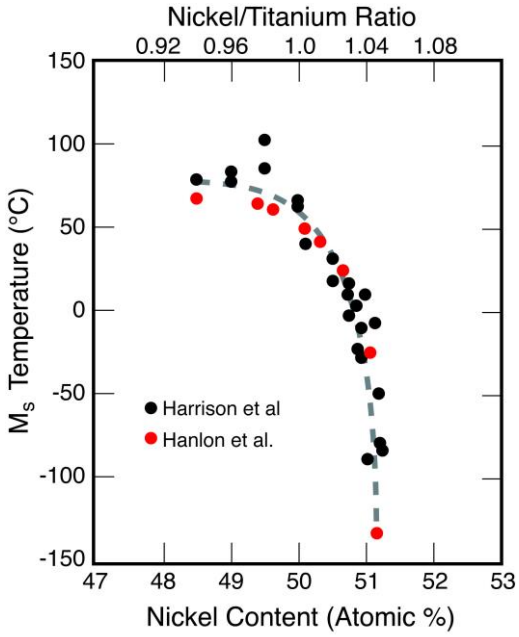

Figure 1. M_s temperature as a function of nickel content [3].

During the production of powder, there is an increase in surface area leading to an increase in oxidation on the surface of the powder. Since various AM processes (e.g., SLM, DED, and electron beam (EB)) all utilize different particle size distributions the oxygen content will vary when making powders for each AM technique. In addition, impurities such as carbon and nitrogen, which can be picked up during melting and atomizing, can influence the A_f temperature. Normally, Nitinol ingots are melted utilizing vacuum induction melting (VIM) or vacuum arc melting (VAR) [4]. The electrode induction melting gas atomization (EIGA[1]) process was used to melt and atomize the powder in this study because it does not use any refractory thereby eliminating contamination from oxides.

It can be seen from the preceding discussion that there are several factors in powder production that impact the transformation temperature. Consequently, a consistent process is needed to be able to predict the transformation temperature of the powder. Even when the powder is produced, the AM process used to fabricate the powder into the final component has an influence on the final transformation temperature. The aim of this paper is to highlight the effect different processing steps can have on Nitinol's transformation temperature from starting ingot to finished part.

Experimental Procedure

Powder Production

The Nitinol powder was produced by gas atomization using a pre-melted and cast bar of Nitinol acquired from Fort Wayne Metals Research Products Corporation. Table I shows the chemical composition of this alloy.

[1]EIGA is a registered trademark of ALD Vacuum Technologies

Table I. Starting ingot chemical composition.

Composition	Ni	Fe	O_2	C	N_2	Cr	Cu	Co	Nb	Ti
[wt%]	55.8	0.012	0.02	0.005	0.004	<0.003	<0.003	<0.003	<0.003	(Balance)

The ingot was converted into powder using the EIGA process shown in Figure 2. EIGA requires bar stock, typically 50-60mm in diameter, as the feed source (precursor material). In this process a Nitinol bar (55mm x 1000mm) is attached to a piston and lowered slowly into an induction coil where the molten metal flows from the tip of the bar into a gas atomizing jet. The atomizing jet uses high purity argon (99.998%) gas to impact the molten metal, convert it to powder, and carry it through the atomizing chamber to a collection hopper. The powder is then screened to the particle size required by the specific AM technique. There are several advantages to the EIGA process in the production of Nitinol. For example, there is little opportunity to volatilize or oxidize the nickel and titanium because the molten metal falls from the bar stock as soon as it reaches its melting point. This leads to nearly full recovery of the nickel and titanium. The process also does not involve any refractory material, so there is no chance of oxide inclusions forming during the melting and atomizing process. Finally, the atomizing and melt chambers are evacuated and then the chambers are filled with high purity argon gas, which minimizes the oxygen and nitrogen pick-up in the powder.

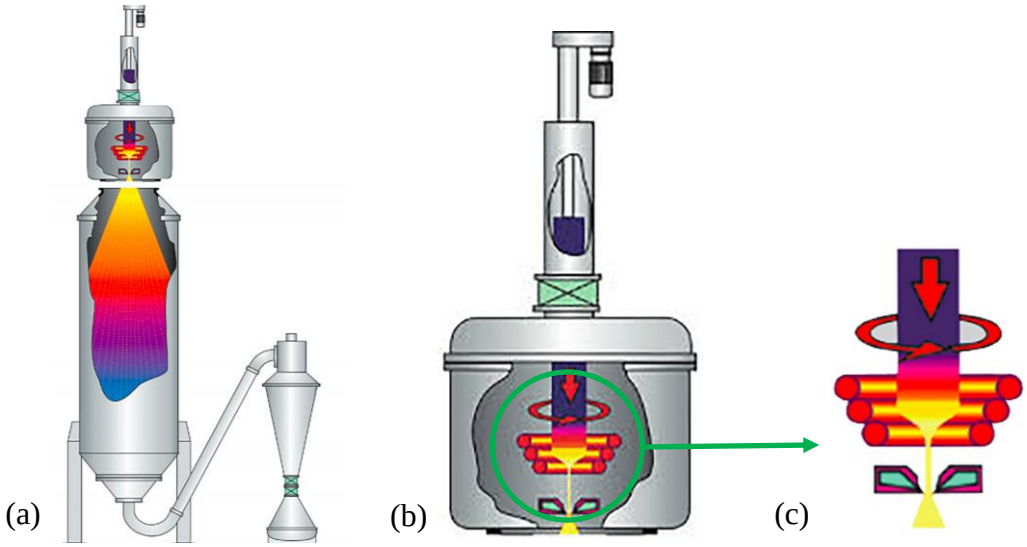

Figure 2. (a) EIGA process showing melting and atomizing chamber, (b) melting chamber and (c) induction coil melting tip of bar and molten metal entering the atomizing chamber [5].

Table II. Particle size distributions of the sieved powder.

Powder	d_{10} [µm]	d_{50} [µm]	d_{90} [µm]
A	11	23	39
B	25	49	88
C	50	70	114
D	104	114	125

The atomized powder was sieved using wire mesh screens and the particle size distributions of the different particle fractions were measured using a Camsizer X2 laser light

scattering system (Table II). Each of the particle size fractions was tested for oxygen, nitrogen, and carbon content using a Leco ONH836 and a Leco CS744. Their transformation temperatures were measured by differential scanning calorimetry (DSC) analysis.

Selective Laser Melting (SLM)

An EOS[2] M290 was utilized to evaluate a range of energy inputs on the A_f transformation temperature due to different process parameter settings. This SLM process works by heating metal powder above its melting point by exposure from an Yb fiber laser within an argon-filled chamber. Process parameter settings can be optimized for the material being printed and correlated to an energy density. Equation 1 shows the formula for energy density where *P* is laser power, *v* is scanning speed, *h* is hatch spacing, and *t* is layer thickness. To study the effect of energy density on chemical composition and the transformation temperature several variations were investigated (Table III).

$$E = \frac{P}{v*h*t} \tag{1}$$

Table III. EOS M290 parameter settings.

	Laser Power [W]	Scanning Speed [mm/s]	Hatch Spacing [mm]	Layer Thickness [mm]	Energy Density [J/mm^3]
Low	250	1200	0.18	0.03	38.6
Medium	280	1200	0.14	0.03	55.6
High	150	500	0.14	0.03	71.4

Re-Melting Experiments

Due to the large amount of effort required to optimize parameters for SLM, powder C (Table II) was also melted into two samples using an Electric Arc Remelt Button Furnace. This experiment provided an extreme condition where the powder was completely re-melted providing a fully dense sample. Smaller pieces were then cut from the samples for further processing and testing. Transformation temperatures were measured using ASTM standard F2004-17 [6].

Heat Treatment

Samples of the atomized powders, SLM produced test samples, and fully melted solids were solution annealed at 850ºC for 15 minutes under argon gas to homogenize the samples and remove any existing precipitate phases and then water quenched to reduce variability [4]. Heat treatments were performed at 350ºC and 450ºC for 1 hour in a tube furnace under argon gas and followed by a water quench. These heat treatment temperatures were chosen because they were shown in previous studies to greatly shift the A_f temperature in Nitinol wire [7]. Transformation temperatures were measured using DSC analysis.

Results & Discussion

Powder was atomized from the starting ingot and sieved to the four different particle size fractions shown in Table II. These particle sizes represent those used in SLM, EB, and DED equipment. Powders used for AM need to be spherical, free flowing and have low internal

[2]EOS is a registered trademark of EOS GmbH

porosity. The particle sizes of powders A and B are typically used for SLM whereas, the particle sizes of C and D are used for DED and EB. Scanning electron micrographs of each of the particle size distributions are shown in Figure 3. The powders are spherical with very few satellites. Table IV shows the circularity and percent porosity of the powders. These values are typical for the particle sizes under consideration.

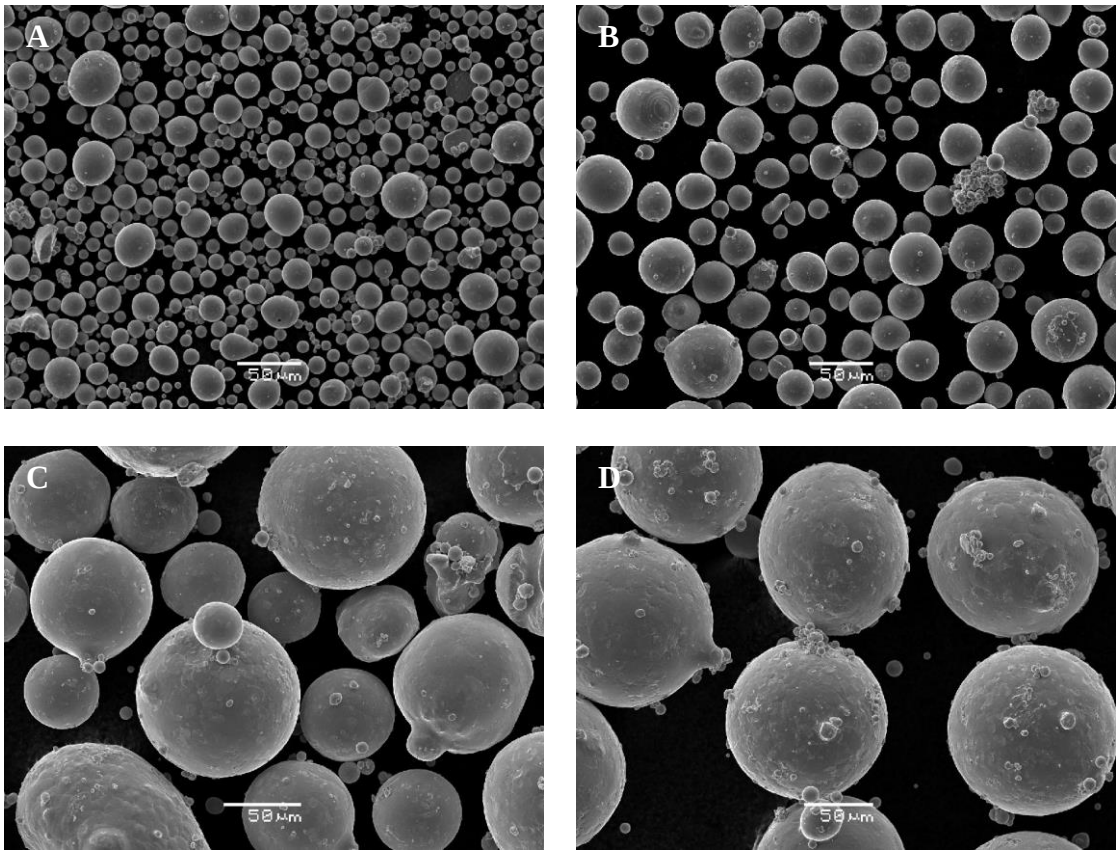

Figure 3. SEM micrographs of powders: A, B, C, & D

Table IV. Measurements of powders.

Powder	d_{50} [µm]	Circularity [µm]	Porosity [%]
A	23	0.85	0.17
B	49	0.82	0.30
C	70	0.82	0.43
D	114	0.78	0.54

The four powders were tested for impurities and transformation temperatures. Table V shows that as the particle size decreased, the A_f temperature decreased as expected, with the upward trend in oxygen content. This is significant as the various AM processes utilize different particles sizes, which result in different transformation temperatures.

Table V. Transformation temperatures & chemical composition of powders.

Powder	d_{50} [µm]	A_f [ºC]	O_2 [wt%]	N_2 [wt%]	C [wt%]
A	23	34	0.045	0.002	0.004
B	49	38	0.033	0.002	0.003
C	70	39	0.026	0.002	0.004
D	114	42	0.023	0.002	0.003

To assess the changes during the SLM process powder C was printed in an EOS M290 machine. Three different energy densities were tested: 38.6 J/mm^3 (low), 55.6 J/mm^3 (medium), and 71.4 J/mm^3 (high).

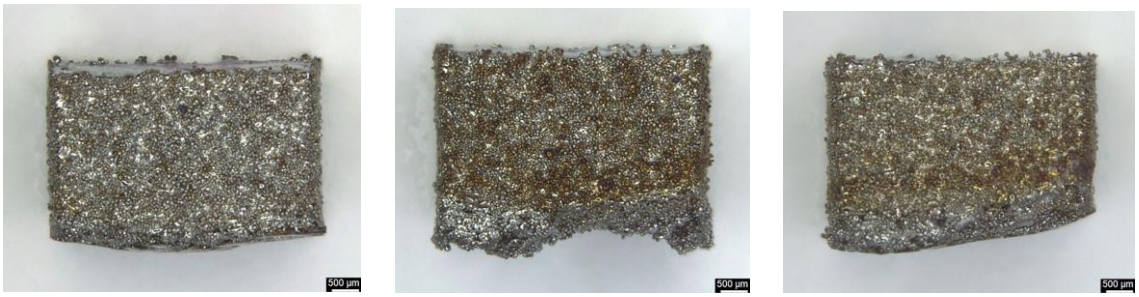

Figure 4. SLM cubes: low, medium, high.

Table VI. EDS results of SLM surfaces.

	Low	Medium	High
Ni [wt%]	52.0	50.8	49.5
O_2 [wt%]	3.23	4.62	5.77

Figure 4 shows the three printed samples. A difference in color can be seen between the low, medium, and high energy densities. Table VI shows the nickel and oxygen concentrations measured by energy dispersive x-ray spectroscopy (EDS) using a scanning electron microscope. The nickel concentration decreased as the energy density increased showing some nickel evaporation took place [8]. There was also an increase in oxygen concentration as the energy density increased. These changes in chemical composition influenced the transformation temperature (Table VII).

Table VII. SLM A_f temperatures.

		Low	Medium	High
As-built	[A_fºC]	54	55	60
Annealed	[A_fºC]	43	44	51
Aged 450ºC	[A_fºC]	48	50	55

Normally in the production of parts from Nitinol, the transformation temperature can be tuned to the desired level by heat treating [7]. The test specimens made from the EOS M290 were subjected to a heat treat cycle that involved annealing the samples then aging at a temperature of 450ºC. For the as-built samples, as the energy density increased, the A_f temperature increased. The annealed samples showed a decrease in the A_f temperature from the

as-built due to precipitates present dissolving and thereby, increasing the nickel content of the matrix [8]. The aged samples showed an increase from the annealed A_f temperature due to the formation of nickel-rich precipitates decreasing the nickel concentration of the matrix [7]. For comparison, fully melted samples were also made from powder C (Table VIII). The fully melted samples showed a more pronounced effect from annealing and aging. Button 2 did not exhibit any transformation temperatures in the as-melted or annealed state. This may be due to the higher oxygen pick-up than button 1 (Table VIII).

Table VIII. Chemical composition of as-built samples and A_f temperatures.

	Button 1	Button 2
As-Melted [A_fºC]	-6	---
Annealed [A_fºC]	-36	---
Aged 350ºC [A_fºC]	27	26
Aged 450ºC [A_fºC]	32	40
O_2 [wt%]	0.07	0.11
N_2 [wt%]	0.02	0.01
C [wt%]	0.02	0.01

The results show there is a large gap between the starting ingot transformation temperature and final part transformation temperature. The ingot began at an A_f temperature of 7ºC and then increased to 39ºC after atomization. The powder was then printed with an energy density of 71.4 J/mm^3 by SLM, which increased it to 60ºC. By annealing, the A_f temperature was brought down to 51ºC and then increased to 55ºC by heat treatment.

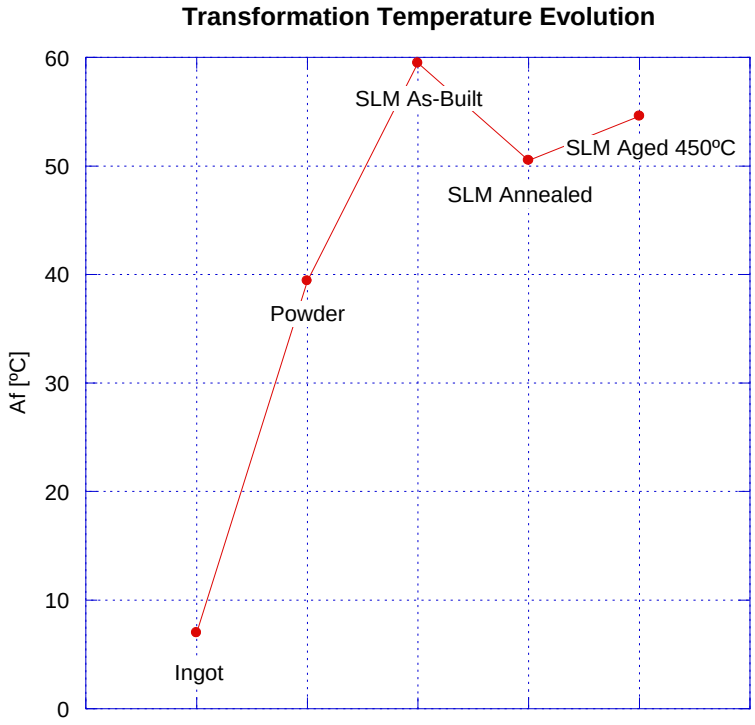

Figure 5. A_f temperature at each process step.

Conclusions

- Particle size influenced the final oxygen concentration of the powder and therefore, the transformation temperature.
- The changes to the chemical composition that occurred during SLM impacted the transformation temperature.
- The results of annealing and heat treating showed that they can be used to manipulate the SLM part's final transformation temperature to a desired level.
- To engineer the appropriate starting powder for an application, each processing step must be taken into consideration from starting ingot to finished part to end up with a targeted transformation temperature.

References

1. A. Wadood, "Brief Overview on Nitinol as Biomaterial," *Advances in Materials Science and Engineering*, vol. 2016, Article ID 4173138, 9 pg.
2. F. Sczerzenie, (2004). Consideration of the ASTM Standards for Ni-Ti Alloys. *SMST-2004: Proceedings of the Second European Conference on Shape Memory and Superelastic Technologies* (203-209). Materials Park, Ohio: ASM International.
3. T. Duerig, K. Melton, D. Stockel, and C. M. Wayman, *Engineering Aspects of Shape Memory Alloys* (Butterworth-Heinemann, 1990), 21-35.
4. Memry, a Saes Group Company. (2017). Introduction to Nitinol. Retrieved June 4, 2018, from https://www.memry.com/intro-to-nitinol
5. ALD Vacuum Technologies GMbH. *Ceramic-Free Metal Powder Production for Reactive and Refractory Metals.* [Brochure] URL. (http://www.ald-dynatech.com/pdf/EIGA.pdf)
6. ASTM F2004-17, Standard Test Method for Transformation Temperature of Nickel-Titanium Alloys by Thermal Analysis, ASTM International, West Conshohocken, PA, 2017.
7. A. Pelton, J. DiCello, S. Miyazaki, "Optimization of Processing and Properties of Medical Grade Nitinol Wire," *Minimally Invasive Therapy and Allied Technologies,* 9(1)(2000), 107-118.
8. S. Saedi, "Shape Memory Behavior of Dense and Porous NiTi Alloys Fabricated by Selective Laser Melting" (Ph.D. thesis, University of Kentucky, 2017).
9. M. Speirs, X. Wang, S. Van Baelen, A. Ahadi, S. Dadbakhsh, J. Kruth, and J. Van Humbeeck, "On the transformation behavior of NiTi Shape-memory alloy produced by SLM," *Shape Memory and Superelasticity*, 2(4)(2016), 310-316.
10. M. T. Andani, "Modeling, Simulation, Additive Manufacturing, and Experimental Evaluation of Solid and Porous NiTi" (M.S. thesis, University of Toledo, 2015).